Measurement of the Yield Stress of Gellike Protein Layers on Liquid Surfaces by Means of an Attached Particle

Jordan T. Petkov* and Theodor D. Gurkov

Laboratory of Chemical Physics Engineering,† Faculty of Chemistry, University of Sofia, James Bourchier Avenue 1, Sofia 1164, Bulgaria

Bruce E. Campbell

Kraft Foods, Inc., Technology Center, 801 Waukegan Road, Glenview, Illinois 60025

Received September 18, 2000. In Final Form: February 7, 2001

We propose a new method for determination of the yield stress of adsorbed protein layers on an air−water interface. A small spherical particle is attached to the surface, and the latter is deformed by pulling up a barrier attached to it. When the tangential projection of the gravity force exerted on the particle exceeds a certain threshold, then the layer starts to undergo significant elastic deformation. This is registered as a difference between the experimentally measured particle displacement and that calculated by solving the Laplace equation of capillarity for the liquid boundary. After the yield threshold, there is a linear dependence of the strain on the applied stress. We propose a modified Bingham model (two springs and a plastic element) to describe this particular rheological behavior. The elastic moduli found by a linear regression analysis of the stress (strain) relationship agree well with literature data for globular proteins. The corresponding yield stress turns out to be very sensitive to changes in the protein layer structure (caused either by the presence of surfactant molecules (Tween 20) or by differences in the bulk protein concentration). The threshold stress monotonically increases with rising protein content, which suggests a possible reinforcement of the adsorbed layer. The addition of Tween 20 brings about surface fluidization. Tween 20 can replace part of the adsorbed protein molecules and/or attach to them breaking the intermolecular linkages.

1. Introduction

The stability and the rheological properties of emulsions and foams are mainly governed by the interactions between the droplets and the air bubbles, respectively.[1] In many food dispersions the stabilizing layers covering either fat droplets or gas bubbles consist of adsorbed molecules of globular milk proteins. The mechanical strength of those layers is one of the factors determining the long-term stability and the stability with respect to mechanical disturbances (e.g., shearing deformation) of the dispersion. The values of the rheological parameters of the surface layers of globular proteins are often orders of magnitude higher than those reported in the literature for low-molecular-weight surfactants or random-coil proteins.[1,2]

Proteins, in general, adsorb strongly and irreversibly at fluid−fluid interfaces (either air−water or oil−water ones), sometimes forming a two-dimensional gellike network. The latter may influence to a considerable extent the dynamic (rheological) properties of the surface.[3−5] Ellipsometry can give valuable information about the thickness of the layer and the amount of adsorbed protein.[6,7] Another source of data for the chemical composition of interfaces, with Angstrom-scale resolution, is the specular neutron reflectivity.[8,9] It provides a detailed picture of the density profile in normal direction to the surface.

If one is interested in revealing the intramolecular and intermolecular interactions at the interface, it is necessary to measure the dynamic response of the protein layer to some external stresses or deformations, sufficiently small in magnitude as to leave the network intact up to a certain limit.[1−10] Description of many different techniques for studying the rheological properties of fluid surfaces can be found in the literature.[2,3,11] Some problems often have to be overcome, in order that one can "read" in a proper way the rheological data. First, the deformation must be well-defined, with clearly distinguishable dilatational and shear components. Second, it is sometimes necessary to consider the hydrodynamic coupling between the motion at the surface and in the underlying solution (see, e.g., ref 12). Also, the mathematical description has to be tractable with viscoelastic layers, which usually form in the case of adsorbed proteins.

* To whom the correspondence should be addressed. E-mail: JP@LTPH.BOL.BG or jpetkov@hotmail.com.

† Formerly: Laboratory of Thermodynamics and Physicochemical Hydrodynamics.

(1) Dickinson, E. *J. Chem. Soc., Faraday Trans.* **1998**, *94* (12), 1657−1669.

(2) Murray, B. S.; Dickinson, E. *Food Sci. Technol., Int.* **1996**, *2* (3), 131−145.

(3) Joly, M. In *Surface and Colloid Science*; Matijevic, E., Ed.; Wiley-Interscience: New York, 1972; Vol. V, p 79.

(4) Graham, D. E.; Phillips, M. C. *J. Colloid Interface Sci.* **1980**, *76* (1), 227, 240.

(5) Izmailova, V. I.; Yampol'skaya, G. P.; Summ, B. D. *Interfacial Phenomena in Protein Systems*; Khimiya: Moscow, 1988; pp 93−115 (in Russian).

(6) de Feijter, J. A.; Benjamins, J.; Veer, F. A. *Biopolymers* **1987**, *17*, 1759.

(7) Holterman, H. J.; 's-Gravenmade, E. J.; Waterman, H. A.; Mellema, J.; Blom, C. *J. Colloid Interface Sci.* **1989**, *128*, 523.

(8) Penfold, J.; Thomas, R. K. *J. Phys.: Condensed Matter* **1990**, *2*, 1369.

(9) Atkinson, P. J.; Dickinson, E.; Horne, D. S.; Richardson, R. M. *J. Chem. Soc., Faraday Trans.* **1995**, *91*, 2847.

(10) de Feijter, J. A. *J. Colloid Interface Sci.* **1982**, *90*, 289.

(11) Edwards, D. A.; Brenner, H.; Wasan, D. T. *Interfacial Transport Processes and Rheology*; Butterworth-Heinemann: Boston, 1991.

(12) Ivanova, M. G.; Verger, R.; Bois, A. G.; Panaiotov, I. *Colloids Surf.* **1991**, *54*, 279−296.

10.1021/la001347i CCC: $20.00
Published on Web 06/23/2001

The interfacial rheology helps to understand the correlation between the layer structure and the macroscopic behavior of the liquid boundary, especially its ability to sustain deformation.[1,2] The latter ability is closely related to the mechanism by which the proteins are believed to stabilize the emulsion/foam films. The exceedingly high viscoelasticity of the film surfaces covered by protein damps the corrugations by fluctuation waves which may lead to rupture;[11] the film drainage is then slow[13] (especially when protein lumps protrude from the interfaces into the aqueous phase); the stiffness of the surface layers prevents drop coalescence when concentrated dispersion (e.g., emulsion cream) is subjected to mechanical disturbances.[14]

Under certain conditions the layers of globular proteins may exhibit purely elastic behavior.[15,16] On the other hand, they may flow and acquire viscoelastic properties.[1,2,4,11,16,17] Basically, this happens when the applied stress is above a certain threshold value, and the transition point carries important information about the molecular interactions within the layer. In general, the physical properties of the protein-laden interfaces change in a broad range, depending on the conditions: type of the protein, presence of low molecular weight emulsifiers, pH of the underlying aqueous phase, temperature, salinity, layer prehistory, and so on.

The rheological measurements reported by other authors (see, e.g., refs 4 and 17) are performed by applying relatively large shear stresses, so that the point of transition from vanishingly small deformation (no macroscopic surface motion) to viscoelastic behavior cannot be discerned. As emphasized by Benjamins & van Voorst Vader,[17] any major deformation partly destroys the protein network at the interface. In the literature the interfacial viscosity and elasticity are usually determined under the conditions of flow, induced by substantial external mechanical impact.[3]

To date, works that concern two-dimensional yield stress are rather scarce. We can mention ref 18; in those works the authors utilized a well-characterized magnetic force in order to obtain information about the limit of protein layer elasticity. They succeeded determining the yield stress of β-casein adsorbed layers, which turned out to be extremely low: $\sim 5 \times 10^{-5}$ mN/m. In contrast, with β-lactoglobulin the respective value was at least 3 orders of magnitude higher: above $\sim 1 \times 10^{-2}$ mN/m. The authors of ref 18 could not measure precisely the yield stress of β-lactoglobulin layers because the upper limit of sensitivity of their instrument was about 1×10^{-2} mN/m, i.e., lower than the value which had to be determined. That is why the method was inapplicable to systems stabilized by globular proteins or proteins forming a strong two-dimensional network, despite its usefulness for very low yield stresses.

Bearing in mind the aforementioned considerations, we tried to create a new method for determination of the yield stress of protein layers. Briefly, we follow the motion of a solid particle which resides on a liquid boundary, when the latter is deformed by pulling up a barrier attached to it. The interface becomes increasingly more inclined, and at sufficiently large slopes the lateral projection of the gravity force exerted on the particle causes it to lag behind the material points on the surface. At that moment, breaking of the protein structure starts. The displacement of the points on the deforming interface is described theoretically, which allows one to extract information about the yield stress of the protein layer from the deviations in the particle position. We are able to apply rather small stresses, starting virtually from zero (when the barrier lies at the level of the plane surface) and increasing them up to a certain limit. A set of experiments have been performed with β-lactoglobulin and Tween 20, with the aim to determine the sensitivity of the layer rheology (and of the method itself) to configurational changes and to the presence of low molecular weight emulsifier.

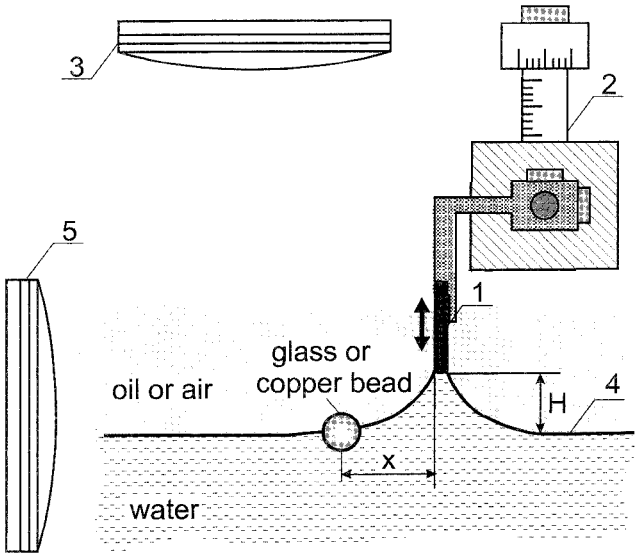

Figure 1. Schematic presentation of the experimental setup. See text for details.

2. Experimental Section

Setup. The apparatus is sketched in Figure 1. It consists of a small circular glass trough, about 10 cm in diameter, where the protein solution is poured in. A glass barrier [1], designed and made hydrophobic, so as to ensure stable catching of the three-phase contact line at its edge, is moved up and down by a micrometric screw table [2]. The motion of the small (submillimeter in diameter) copper bead is observed through the vertical microscope [3] and by a CCD camera (not shown in Figure 1). Although the final results are not very sensitive to the particle three-phase contact angle, in our calculations we have used the correct contact angles measured precisely (experimental error less than 5%) by means of the horizontal microscope [5] shown in Figure 1. Records are taken by means of a VCR.

Materials and Experimental Procedure. Bovine β-lactoglobulin was obtained from Sigma (St. Louis, MO), catalog # L-0130, lot # 124H7045. It was a mixture of genetic variants A and B. High purity polyoxyethylene (20) sorbitan monolaurate (Tween 20) was also purchased from Sigma. As a hydrophobizing reagent (for treating the glass barrier prior to each experiment) we applied hexamethyldisilazane (Sigma). In all our experiments we worked at the "natural" pH (6.2−6.3), a value resulting when β-lactoglobulin was dissolved in water, without any additives for control of pH. We used Milli-Q ultrapure water (Millipore, USA) to prepare all aqueous solutions.

(13) Ivanov, I. B.; Dimitrov, D. S.; Thin Film Drainage, In *Thin Liquid Films*; Ivanov, I. B., Ed.; Marcel Dekker: New York, 1988; Chapter 7, p 379.

(14) Dimitrova, T. D.; Gurkov, T. D.; Vassileva, N. D.; Campbell, B.; Borwankar, R. P. Kinetics of Cream Formation by the Mechanism of Consolidation in Flocculating Emulsions. *J. Colloid Interface Sci.*, in press.

(15) Petkov, J. T.; Gurkov, T. D.; Campbell, B. E.; Borwankar, R. P. *Langmuir* **2000**, *16* (8), 3703−3711.

(16) Gurkov, T. D.; Petkov, J. T.; Campbell, B. E.; Borwankar, R. P. Food Colloids 2000: Fundamentals of Formulation. Dilatational and Shear Rheology of Protein Layers on Water/Air Interface; Proceedings of the Conference; April 2−5, 2000, Potsdam, Germany; Dickinson, E., Miller, R., Eds.; Royal Soc. Chem.: Cambridge, UK, in press.

(17) Benjamins, J.; van Voorst Vader, F. *Colloids Surf.* **1992**, *65*, 161−174.

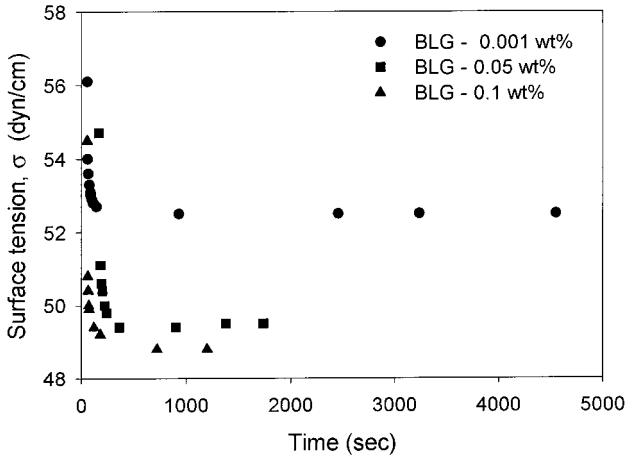

Figure 2. Surface tension isotherms of β-lactoglobulin (BLG) solutions. The experiments were performed at natural pH (~6.2), with no electrolyte added, at room temperature ($T = 22$ °C).

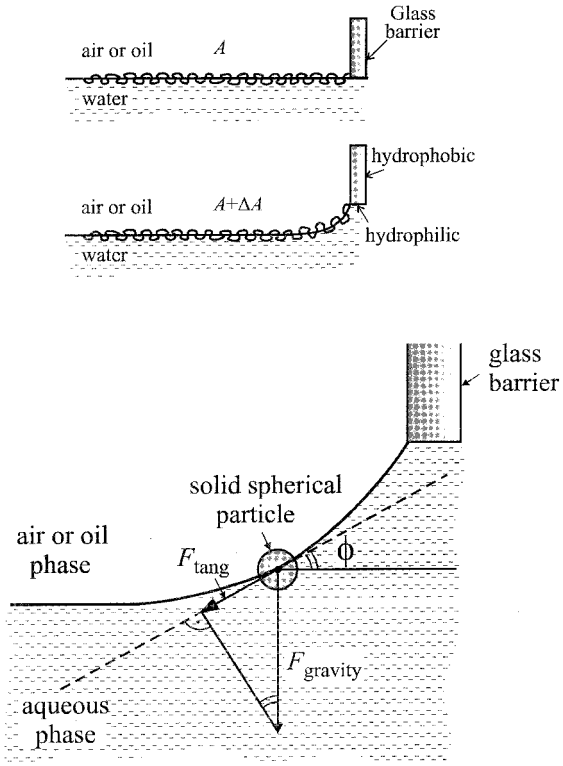

Figure 3. Sketch of the adsorbed protein layer before and after deformation, the geometry when a spherical particle is attached to the deformed surface, and the applied force.

The experimental procedure starts with pouring the protein solution into the glass dish. It is then left for 30 min for the surface tension to reach a quasi-equilibrium value (i.e., to stop changing appreciably). At the studied protein concentrations the adsorption kinetics is rather fast, see Figure 2, so 30 min are sufficient for establishment of surface/bulk diffusion equilibrium. After that, small ballotini are gently placed on the liquid boundary with the help of a specially designed glass holder.

In general, when the interface is deformed upward by means of the glass barrier, the particle, due to the tangential projection of the gravitational force, has to recede away from the barrier if its motion is free, see Figure 3. However, the interface is highly elastic, as a result of protein adsorption and subsequent unfolding in a strongly cohesive and entangled layer. For this reason, upward movement of the barrier does not lead to retreat of the particles. On the contrary, displacement *toward* the barrier is observed. The phenomenon will be explained in more details in the next section. We have made a series of experiments elevating the barrier and stretching the interface in that way, see Figure 3, with subsequent return of the barrier to its horizontal position. By reading the height of elevation and recording the respective particle displacement, we follow the response of the interface to the applied stress. About 30 different experimental runs are usually performed with the same protein layer. Later, the images are processed frame by frame and the exact particle positions are accounted, before and after stretching of the layer.

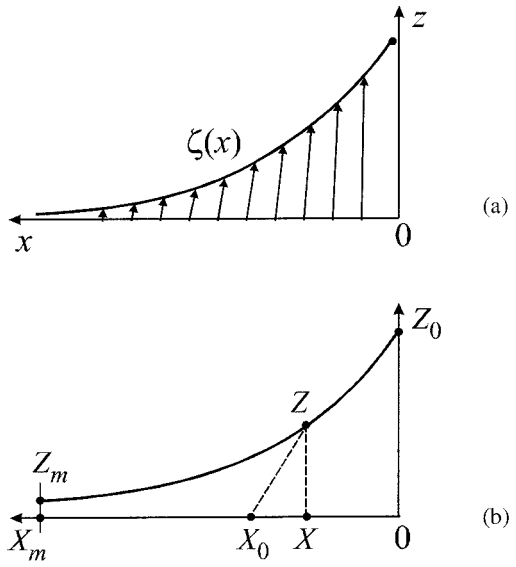

Figure 4. Scheme of the meniscus profile during deformation. (a) Displacement of the material points. (b) Notation for the coordinates of points (see text for details).

3. Theory

We need to investigate the kinematic effect of the motion of the interfacial material points due to the expansion of the liquid boundary. In the geometry of the raised meniscus (see Figures 1, 3, and 4) there is a translational symmetry (in the direction perpendicular to the drawings), and the extensional deformation is "uniaxial" (along the x-coordinate).

We may write the general condition for mechanical equilibrium of the curved interface (i.e., the stress balance):

$$\nabla_s \cdot \mathbf{T}_s + \Delta P \mathbf{n} = 0 \qquad (1)$$

where ∇_s is the two-dimensional surface gradient operator, $\mathbf{T}_s$ is the surface stress tensor, ΔP is the local hydrostatic pressure difference, and $\mathbf{n}$ is the outer unit normal to the interface. We assume that $\mathbf{T}_s$ has two nonzero components (eigenvalues), σ_1 and σ_2, $\mathbf{T}_s = \mathbf{e}_1\mathbf{e}_1\sigma_1 + \mathbf{e}_2\mathbf{e}_2\sigma_2$, where $\mathbf{e}_1$, $\mathbf{e}_2$ are orthogonal unit vectors tangential to the surface. The latter equation is valid when the protein layer exhibits viscoelastic properties. Then, one has to bear in mind that the interfacial tension is a tensorial quantity. (Due to the fact that the deformation is uniaxial, there will be no contributions of type $\mathbf{e}_1\mathbf{e}_2\sigma_{12}$ to $\mathbf{T}_s$.) For the time being, we also account for the possibility that gradients of σ_1, σ_2 might exist, $\sigma_1 = \sigma_1(x)$, $\sigma_2 = \sigma_2(x)$.

Equation 1 can be resolved into horizontal (along x) and vertical (along z) components (x and z are Cartesian coordinates, Figure 4a). If $\zeta(x)$ is the local elevation of the surface, then $\Delta P = -\Delta\rho g\zeta(x)$, with $\Delta\rho > 0$ being the density difference and g the acceleration due to gravity. The resulting stress balances read:

$$\left[\begin{array}{ll} -\dfrac{1}{\tan\phi(x)}\ \dfrac{\mathrm{d}}{\mathrm{d}x}[\sigma_1(x)\cos\phi(x)] = \Delta\rho g\zeta(x) & \text{horizontal} \\ \dfrac{\mathrm{d}}{\mathrm{d}x}[\sigma_1(x)\sin\phi(x)] = \Delta\rho g\zeta(x) & \text{vertical} \end{array}\right] \tag{2}$$

where $\phi(x)$ is the running slope angle (i.e., $\tan\phi(x) = \mathrm{d}\zeta/\mathrm{d}x$). The component σ_2 has disappeared from the balances, and the two equations (2) are consistent only if $(\mathrm{d}\sigma_1/\mathrm{d}x) = 0$. We arrive at the important conclusion that in mechanical equilibrium there can be no lateral gradient of σ_1 , and therefore, the dilatational deformation is *homogeneous* (uniform) throughout the interface. For the sake of brevity, in our further considerations we will omit the subscript "1" of σ_1 , i.e., $\sigma_1 \equiv \sigma$.

Dimensionless variables are now introduced by scaling ζ and x with the capillary length, L:

$$X \equiv \frac{x}{L}, \quad Z \equiv \frac{\zeta}{L}, \quad L = \sqrt{\frac{\sigma}{\Delta\rho g}} \tag{3}$$

With

$$\sin\phi = \frac{\tan\phi}{\sqrt{1+\tan^2\phi}} = \frac{Z'}{\sqrt{1+Z'^2}}, \quad Z' \equiv \frac{\mathrm{d}Z}{\mathrm{d}X} \tag{4}$$

eq 2 is transformed to read

$$Z'' = Z(1+Z'^2)^{3/2} \tag{5}$$

Equation 5 can easily be solved analytically. The first integration is taken using the boundary condition that $Z' = 0$ should hold wherever $Z = 0$ (that is, at $X \to \infty$). Then eq 5 gives

$$\frac{\mathrm{d}Z}{\mathrm{d}X} = \frac{Z\sqrt{4-Z^2}}{Z^2-2} = Z' \tag{6}$$

In our particular configuration $Z' < 0$, and eq 6 is valid only for $Z < \sqrt{2}$. The meniscus becomes vertical at $Z = \sqrt{2}$. The integration of eq 6 is carried out with the boundary condition $Z = Z_0$ at $X = 0$ (Figure 4b). The final result is

$$X = \sqrt{4-Z_0^2} - \sqrt{4-Z^2} + \log\left\{\frac{Z_0}{Z}\,\frac{2+\sqrt{4-Z^2}}{2+\sqrt{4-Z_0^2}}\right\} \tag{7}$$

which represents the explicit solution for the interfacial profile.

Now we wish to find the area of the deformed surface. Let $\mathrm{d}A$ be an elementary parcel, whose width (in a direction perpendicular to the drawing in Figure 4) is an arbitrary length l. Then

$$\frac{\mathrm{d}A}{Ll} = \sqrt{1+Z'^2}\,\mathrm{d}X, \quad \frac{A}{Ll} = \int_0^X \sqrt{1+Z'^2}\,\mathrm{d}X \tag{8}$$

Here A denotes the interfacial area enclosed from the point $X = 0$, $Z = Z_0$ to the point (X, Z) in Figure 4b. We switch to variable Z in the integral, substituting Z' from eq 6. Straightforward calculation yields

$$\frac{A}{Ll} = \log\left\{\frac{Z_0}{Z}\,\frac{2+\sqrt{4-Z^2}}{2+\sqrt{4-Z_0^2}}\right\} \tag{9}$$

A dilatational parameter, α, can be defined as $\alpha \equiv A/A_0$, where A_0 is the initial area of the surface parcel under consideration, in its planar state before deformation. In the present work we will need to analyze only cases where the interface exhibits purely elastic rheological behavior, i.e., where viscous flow does not occur at all. Experimentally, such behavior has been confirmed with layers of globular proteins under certain conditions (see ref 15, Figures 6 and 8, and the next section). We are actually interested in finding the point where the interface starts to undergo significant deformation under the action of a stress of increasing magnitude (i.e., when yielding occurs).

As has already been proven, the expansion is homogeneous and α will be independent of the X coordinate, but of course will depend on the barrier elevation Z_0, Figure 4b. The combination of eqs 9 and 7 leads to

$$X = \sqrt{4-Z_0^2} - \sqrt{4-Z^2} + \alpha X_0 \tag{10}$$

where $X_0 = (A_0/Ll)$ denotes the initial position (on the flat nondeformed surface) of the material point whose horizontal coordinate on the curved meniscus is X (cf. Figure 4b). Equation 10 can be applied to the end point $(X_\mathrm{m}, Z_\mathrm{m})$, which does not move horizontally upon elevation of the barrier (Figure 4b). In a rectangular trough the point $(X_\mathrm{m}, Z_\mathrm{m})$ pertains to the wall; the quantity $z_\mathrm{m} = Z_\mathrm{m} L$ represents the height of the meniscus at $x_\mathrm{m} = X_\mathrm{m} L$, accounted from the level which would have been reached by the surface at $x \to \infty$. In a more complicated geometry of the vessel (e.g., circular one) the point $(X_\mathrm{m}, Z_\mathrm{m})$ is purely fictitious, with X_m being a model parameter. The calculations are not sensitive to the actual size of the container (or to X_m), because the whole area (A, A_0) is much larger than the characteristic region of elevated meniscus where the deformation is appreciable. By means of suitable rearrangement of the expression (10) and substitution with eq 7 (written for $X = X_\mathrm{m}$, $Z = Z_\mathrm{m}$), we end up with

$$\alpha = \frac{1}{X_\mathrm{m}}\log\left\{\frac{Z_0}{Z_\mathrm{m}}\,\frac{2+\sqrt{4-Z_\mathrm{m}^2}}{2+\sqrt{4-Z_0^2}}\right\} \tag{11}$$

This equation will be used for determination of α at each particular value of Z_0. A relation between X_0, α, Z_0, and Z is attained from eqs 10 and 7:

$$Z = \frac{4B}{B^2+1}, \quad B \equiv \frac{2+\sqrt{4-Z_0^2}}{Z_0}\exp(\alpha X_0) \tag{12}$$

We implement the following computational algorithm: (i) arbitrary value is assigned to X_m (usually x_m is chosen to be the size of the glass trough); (ii) for a certain experimental Z_0 we determine Z_m by numerical solution of the nonlinear eq 7 (written for $X = X_\mathrm{m}$, $Z = Z_\mathrm{m}$); (iii) the dilatational parameter α is found from eq 11; (iv) for a chosen initial position of a material point, X_0, we find the Z-coordinate of that point in the deformed state of the interface, using eq 12; (v) the resulting Z is plugged into eq 7 and the corresponding horizontal coordinate X is finally obtained. In this manner we compute the displacement $(X_0 - X)$ of any point for a given barrier elevation Z_0.

There is a complication here, which arises from the fact that in principle the interfacial tension, σ, depends on the expansion α. For pure elasticity one has

$$d\sigma = E_G \frac{dA}{A}, \quad \sigma(A) = \sigma(A_0) + E_G \log\frac{A}{A_0} \qquad (13)$$

for arbitrary deformations. We assume that the Gibbs elasticity, $E_G \equiv d\sigma/d \log A$, is constant. If $A - A_0 \ll A_0$, eq 13 may be presented in the form

$$\sigma = \sigma_0 + E_G(\alpha - 1) \qquad (14)$$

where $\sigma_0 \equiv \sigma(A_0)$. The height z_0 is measured experimentally, but it cannot be immediately scaled to a dimensionless quantity because we do not know $\sigma(\alpha)$ a priori. (The same holds also for the distances x_m and x_0.) Indeed, L itself is a function of α through σ (cf. eq 3). For this reason, we adopt an iterative scheme: as a zeroth-order approximation we take z_0, x_m, and x_0 normalized by $L(\sigma_0)$. Next, we determine α by the procedure described above and find a corrected value of the interfacial tension, $\sigma_{(1)}$. A new normalization of z_0 , x_m, and x_0 is then made by $L(\sigma_{(1)})$, new values of α and σ are found, and so on. This procedure is rapidly convergent, within just a few iterations.

In the present paper the theoretical curves were calculated by disregarding the effect of E_G (i.e., by putting $E_G = 0$). We have verified that if the overall surface area is large enough, then α is very close to 1 (in our systems typically $\alpha \sim 1.01$). Then, values of E_G up to hundreds of dynes per centimeter are immaterial because the profile is insensitive to such small changes of σ (cf. eq 14). In addition, the exact value of x_m is also irrelevant; for the same reason, $A - A_0 \ll A_0$. In some cases we have chosen $x_m = 10$ cm. Still, our theoretical treatment fully includes the effect of E_G and the finite size of the container, x_m. These details may be needed if one decides to make a substantial expansion of the liquid interface, e.g., by means of a laterally moving barrier in a Langmuir trough.

4. Results and Discussion

Figure 5 illustrates the ability of a particle to follow the motion of the surface material points when the protein layer is stretched. The particle displacement, Δx (initial minus final horizontal position, $x_0 - x_f$), is plotted as a function of the height of barrier elevation, H. The latter is taken with respect to the "zero" level of the surface far away from the barrier; see Figure 1. Δx is defined as the difference in the positions of the particle when the interface is not deformed (i.e., when the barrier lies at the same level as the flat liquid boundary) and when it is deformed.

The symbols in Figure 5 stand for the experimentally measured particle displacements, while the solid lines represent theoretically calculated displacement of the interfacial material points which have been lying initially at the same lateral distance x_0 from the barrier as the particle. To calculate those curves in Figure 5, we used the following parameters: $\sigma = 52.5$ dyn/cm for 1 x 10^{-3} wt % β-lactoglobulin, Figure 5A, $\sigma = 49.2$ dyn/cm for 0.05 wt % β-lactoglobulin, Figure 5b, and $\sigma = 48.8$ dyn/cm for 0.1 wt % β-lactoglobulin, Figure 5c; $E_G = 0$ dyn/cm; trough length $x_m = 10$ cm; $\Delta\rho = 1$ g/cm^3 (at air−water interface). We have to emphasize once again here that the results are absolutely insensitive to the values of E_G and the trough length. Therefore, in fact *no adjustable parameters* are involved in the calculation of the theoretical displacement curves.

Increasing deviation of the experimental points from the lines in Figure 5 are observed for heights greater than certain values, H_{cr}. This reflects the partial loss of layer rigidity, which happens after a sufficiently large external force (gravity projection, F_{tang}, Figure 3) is applied on the particle. At this moment the particle can no longer move together with the interfacial material points (and act simply as a marker) but starts to lag behind.

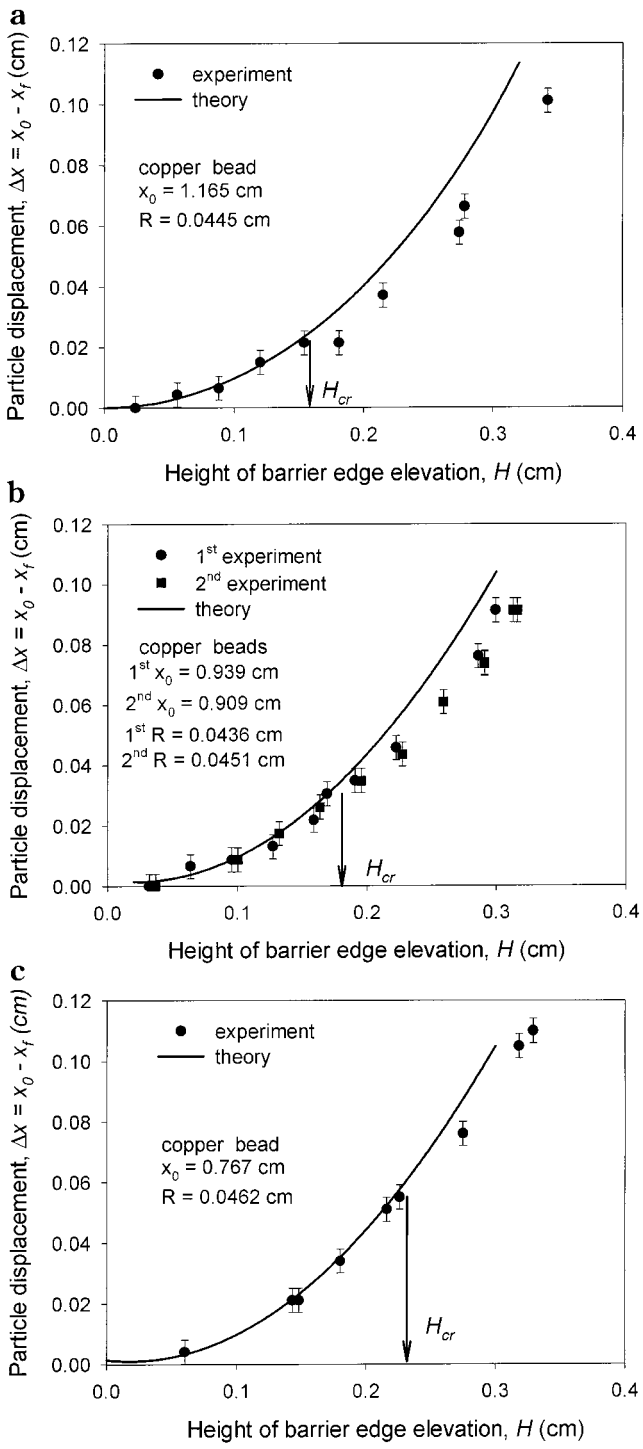

Figure 5. Typical experimental results for particle displacement upon layer stretching. The solid symbols represent experimental points (particle positions), while the solid line is the solution of the Laplace equation of capillarity (positions of the surface material points). The system contains: (a) 0.001 wt % β-LG; (b) 0.05 wt % β-LG; (c) 0.1 wt % β-LG. No electrolyte was added; the pH was natural (6.2); $T = 22$ °C.

Comparing the data in parts a−c of Figures 5, we see that there exists a pronounced effect of the protein content on the point where the layer becomes less rigid and starts to undergo significant deformation. The higher the protein bulk concentration, the greater the height of barrier

elevation, H_{cr}, at which this transition occurs. Our observation is in consonance with data reported by Dickinson and co-workers.[9] They used a very powerful method for studying the chemical composition and thickness of protein layers: specular neutron reflectivity. The measured thicknesses of protein layers were 10.2 ± 1.0 and 12.7 ± 1.1 nm, corresponding to bulk concentrations of 1 x 10^{-3} and 0.1 wt % BLG, respectively. Hence, with more protein the higher rigidity, manifested as higher H_{cr} for yielding, can reasonably be correlated with larger thickness of the layer. Another explanation could be sought in the increased amount of adsorbed protein as pointed out by van Vliet et al.[18] By ellipsometry measurements they have observed that the increase of the volume fraction of the protein in the bulk leads to increased adsorption accompanied with a decrease of the layer thickness. Taking into account the data of Dickinson and co-workers it might be that both effects contribute to the overall layer strengthening: increased amount of adsorbed protein and thickening of the layer.

In Figure 6 we plot the difference between the experimentally measured particle displacement, Δx_{exp}, and the theoretically predicted displacement of the surface material points, Δx_{th}. The quantity $(\Delta x_{th} - \Delta x_{exp})$ is normalized by the initial position x_0 and is represented as a function of the tangential force per unit length of the three-phase contact line perimeter (cf. Figure 3). r_c denotes the radius of the wetted circumference on the spherical particle. Figure 6a refers to a system containing 1 × 10^{-3} wt % β-LG at the natural pH, without added electrolyte. The points are shown with their experimental error (bars). It is seen that two well-defined regions can be discerned. The initial portion of the plot at small stresses is a horizontal line with $\Delta x_{th} - \Delta x_{exp} = 0$. This indicates full coincidence of the particle displacement with the displacement of the surface material points. In other words, the particle serves just as a marker on the interface. Obviously, the force acting on the particle has a very small magnitude, insufficient to cause breakage of the intermolecular links, so that the layer resists deformation. Following the same way of representing the data, we plot in Figure 6b,c the respective dependencies for different concentrations of β-LG: 0.05 and 0.1 wt %.

After a certain critical stress, corresponding to the value F_{tang}^{cr}, the layer behavior changes: the tangential projection of the gravity force overcomes the layer stiffness, and a significant deformation occurs. The difference between the experimentally measured particle displacement, Δx_{exp}, and the value Δx_{th} predicted for the interfacial material points grows up with the stress—see the right-hand linear branches of the curves in Figure 6. We believe the rheological behavior of the layer in this second region is elastic, for the following two reasons: first, after such a stretching with a particle lag, we still do observe reestablishment of the initial particle position, x_0, when the barrier is returned to its initial position at the level of the flat liquid boundary; second, the connection between the strain and the stress is linear, which implies Hookean elasticity.

From the intersection points of the two linear portions of the plots for different protein solution concentrations, we determine the critical force for yielding (per unit length); the data are collected in Figure 7 (several experimental values were averaged for each concentration). It is not surprising that the bigger the protein concentration, the larger the critical force. This result is in agreement with data found in the literature:[9,19] the authors have reported that the layer density increases as the bulk protein concentration rises. It is likely that more dense layers would exhibit improved stiffness.

Values for the critical tangential force obtained by us are in qualitative agreement with the findings of van Vliet

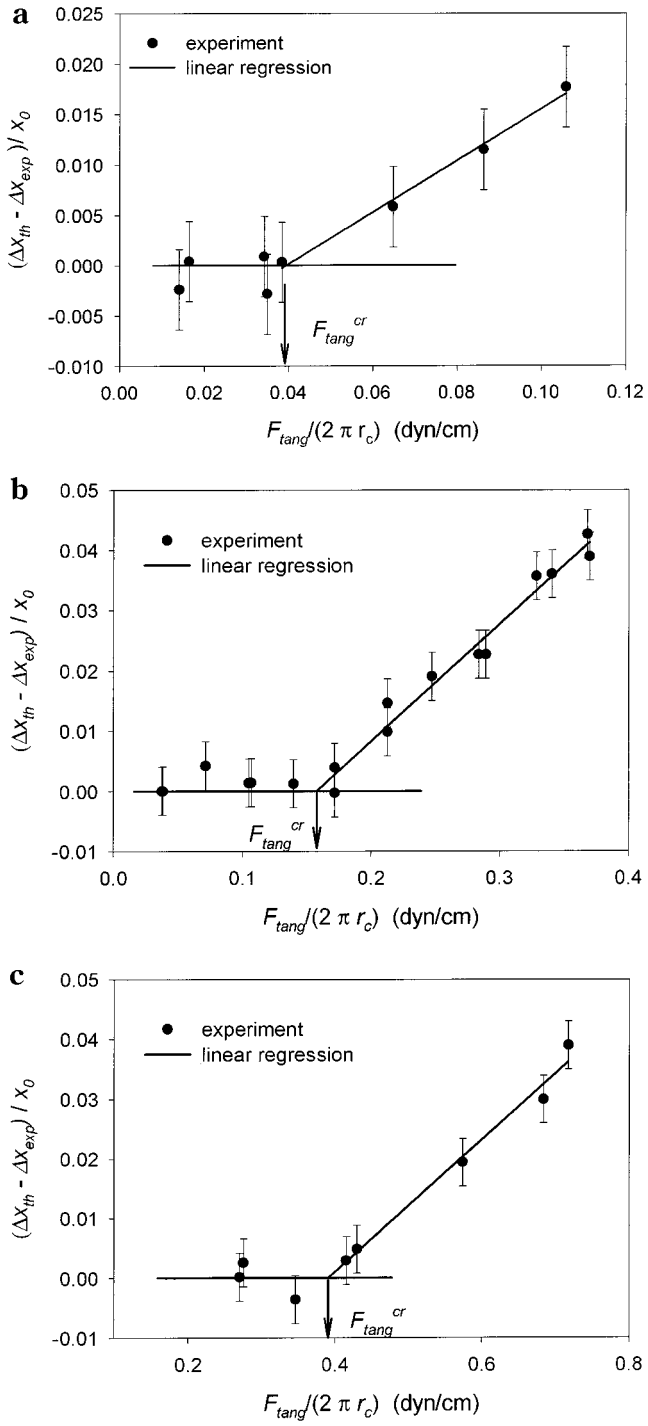

Figure 6. Dependence of the strain in the layer on the applied stress. $\Delta x_{th} - \Delta x_{exp} = 0$ means that the particle follows exactly the displacement of the surface material points (and thus just serves as a marker). The system contains: (a) 0.001 wt % β-LG; (b) 0.05 wt % β-LG; (c) 0.1 wt % β-LG. No electrolyte was added; the pH was natural (6.2); T = 22 °C.

(18) van Vliet, T.; de Groot-Mostert, A. E. A.; Prins, A. *J. Phys. E: Sci. Instrum.* **1981**, *14*, 745−746. Boerboom, F. J. G.; de Groot-Mostert, A. E. A.; Prins, A.; van Vliet, T. *Netherlands Milk Dairy J.* **1996**, *50*, 183−198.

(19) Eaglesham, A.; Herrington, T. M.; Penfold, J. *Colloids Surf.* **1992**, *65*, 9.

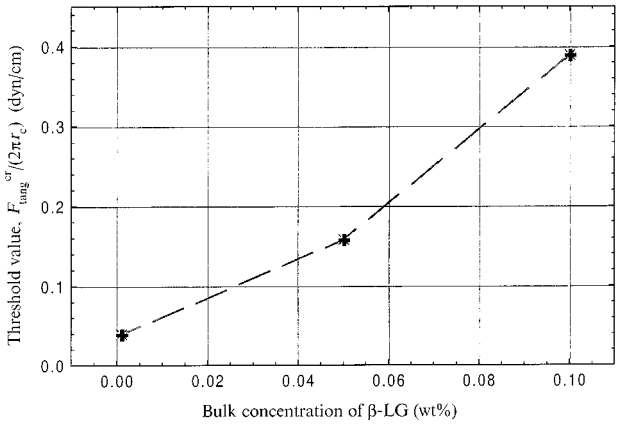

Figure 7. Concentration dependence of the yield threshold stress in adsorbed protein layers.

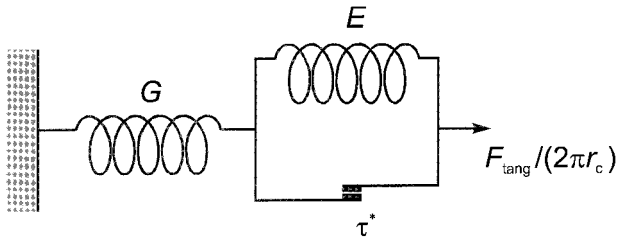

Figure 8. Modified Bingham's body. Instead of a Newton dashpot, it contains a spring with elastic modulus E, connected parallel to a plastic element.

and co-workers,[18] who have determined the "yield stress" of adsorbed BLG layers at the air−water interface to be *higher* than 0.01 dyn/cm. The lowest value of the yield stress extracted from our experiments is 0.039 dyn/cm for the system containing 0.001 wt % BLG. The latter value is above the limit of applicability of the method employed in ref 18.

The linear relationship between the applied stress and the strain, demonstrated by the right-hand branches of the plots in Figure 6, suggests that the rheological behavior could be described by a model with plastic and elastic elements. We modify the well-known Bingham rheological model to obtain the scheme shown in Figure 8. An elasticity G (of high value) is responsible for the layer stiffness before macroscopically appreciable deformation can develop. A second Hookean elastic element with modulus E is connected to the plastic element, whose characteristic yield stress is τ^*. While

$$\frac{F_{tang}}{2\pi r_c} < \tau^* \qquad (15)$$

the plastic element is inactive (Figure 8), and only the first spring (G) is operative. As its elasticity is supposedly high (corresponding to strong intermolecular linkages), no deformation of the layer could be detected and $\Delta x_{th} - \Delta x_{exp} \approx 0$ (see the horizontal lines in Figure 6). Once the threshold stress τ^* is overcome ($\tau^* = F_{tang}^{cr}/(2\pi r_c)$), the second spring ($E$) starts to deform (this corresponds to the second linear region in Figure 6). We define the effective elasticity modulus, E, as the slope of the stress $F_{tang}/(2\pi r_c)$ vs strain $(\Delta x_{th} - \Delta x_{exp})/x_0$ dependence (Figure 6). The values of E are listed in Table 1, where the obtained results are compared with data of Benjamins and van Voorst Vader[17] for bovine serum albumin. We can say that the agreement is good, bearing in mind how complex the protein systems are, and that even results with the same

Table 1. Experimental Data for the Effective Elasticity Modulus of BLG and BSA Layers on A/W Boundary

BLG, wt %	1×10^{-3}	5×10^{-2}	1×10^{-1}
E, dyn/cm	3.9	5.1	9.0
BSA,[a] wt %	1×10^{-4}	5×10^{-4}	1×10^{-2}
E,[a] dyn/cm	3.5	6.8	5.0

[a] Reference 17.

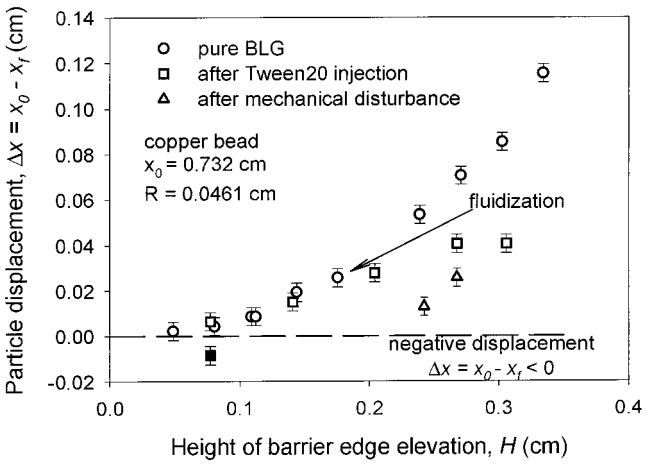

Figure 9. Effect of inclusion of low molecular weight surfactant, Tween 20, on the protein layer elastic properties. See text for details.

protein obtained by one and the same method very often differ considerably.[17] The linearity between the applied stress and the strain, as well as the precise (in the framework of the experimental error) reestablishment of the initial position, x_0, suggest that we deal with a protein layer showing elasticity above a certain value of the applied force. There is no "fluidization", at least not until low molecular weight surfactant is added.

Effect of Low Molecular Weight Nonionic Surfactant, Tween 20. Figure 9 illustrates the behavior of a copper sphere placed initially in a layer adsorbed from a 0.1 wt % solution of BLG. After performing about 30 runs of stretching of the pure protein layer (see the empty circles), we injected 0.5 mL of Tween 20 solution, so as to reach an overall surfactant concentration of 1×10^{-5} M. The final Tween-to-protein molar ratio was equal to 0.2. After the addition of the low molecular weight surfactant, we waited about 5 min before continuing the layer stretching. It is worthwhile to mention that the stretching was conducted by a gradual increase of the height of elevation of the barrier edge, until a difference was detected between the particle displacements before and after Tween 20 addition. A very important observation has been made: the initial position of the particle cannot be reestablished when the barrier is returned to the flat liquid level, which indicates loss of Hookean elasticity and partial fluidization of the layer. Most probably, due to the inclusion of small molecules inside the protein network, the structure of the latter is destroyed, and some of the intermolecular bonds formed during the unfolding process are broken.

Different authors have studied the effect of low molecular weight emulsifier on the properties of protein films and the consequences for the overall emulsion stability.[20−25] Dickinson and Gelin[21] report that if the low molecular

(20) Mackie, A. R.; Gunning, A. P.; Wilde, P. J.; Morris, V. J. *J. Colloid Interface Sci.* **1999**, *210*, 157.
(21) Dickinson, E.; Gelin, J.-L. *Colloids Surf.* **1992**, *63*, 329.
(22) Chen, J.; Dickinson, E. *Colloids Surf.* **1995**, *100*, 255; 267.
(23) Chen, J.; Dickinson, E. *Colloids Surf.* **1995**, *101*, 77.

weight surfactant is in a high enough concentration, it fully ousts the protein molecules within a time period of seconds to minutes. In our experiments the Tween 20 content is low. Correspondingly, the aging time needed for appearance of significant effect on the rheological properties of the layer is relatively longer.

Another interesting point is that the layer, if left mechanically untouched, still demonstrates appreciable elasticity even in the presence of Tween 20. If, however, we damage the surface layer mechanically (e.g., by puncturing it with a glass stick), the interface starts to "flow" and the particle displacement toward the barrier becomes very small; see Figure 9 (the triangles). It is likely that the ability of Tween 20 to replace the protein or connect to it greatly augments once the surfactant molecules get on the interface. Dickinson and Euston[26] point out that even at very low surfactant concentration, well below that required for a substantial protein displacement, the protein surface rheology is affected tremendously. Results on surface shear viscosity of β-lactoglobulin layers in the presence of Tween 20 (ref 27) confirm this strong influence. Considered in the light of our own observations with β-lactoglobulin and Tween 20, before and after a mechanical disruption, we would say that surface shear viscosity measurements are connected with large uncertainty when it comes to mixtures of proteins and low molecular weight surfactants. This is due to the impact of the mechanical prehistory: what is believed to be the surface shear viscosity will be strongly influenced by the mechanical disturbance of the measuring body (e.g., disk, ring, knife-edged bob, etc.). An indirect corroboration of that can be seen in the behavior of the layer from Figure 9. The solid square point reflects the displacement of the copper particle at a certain height of barrier elevation immediately after the mechanical intervention. The layer exhibits almost full fluidity, as the particle translates away from the barrier (cf. also Figure 3).

Our brief comment on this phenomenon is that it is important whether a mixed layer is formed during simultaneous adsorption of both components (low molecular weight surfactant and protein) or this competitive adsorption takes place after the protein layer has already been formed. Especially at low emulsifier-to-protein ratios, the secondary surfactant adsorption is more or less hindered by the strongly cohesive protein network. If, however, we mechanically force the intermolecular protein bonds to break, the surfactant adsorption quickly progresses giving a new, less elastic, interfacial layer. In the case when the low molecular weight emulsifier competitively adsorbs together with the protein from a mixed solution, no matter what the protein concentration is, the resulting layer is always highly fluid, with total lack of Hookean elasticity. Even the slightest attempt to stretch the adsorbed layer makes the particle to recede away from the barrier (cf. Figure 3).

We checked the interfacial tension kinetics in mixed systems, comparing it with the case of Tween 20 alone. The results are not shown in detail here, but it is sufficient to say that the equilibrium value of the surface tension of the mixtures does not differ from that of a pure solution of Tween 20 with the same concentration (5×10^{-5} M). This fact does not mean that the layer is devoid of protein; it confirms the dominant role of the more surface active Tween 20 molecules, whose surface pressure is much greater than that of the big protein globules of BLG. The recently reported "orogenic" mechanism of protein displacement by surfactant includes compression of the protein under the increased surface pressure of Tween.[20] Another evidence of how the small surfactant molecules behave on the interface is given in ref 15. If on an adsorbed layer of BLG we drop a minute amount of Tween 20 solution, due to the high surface pressure of the surfactant molecules, within less than a second the surface tension, σ, changes to that of a pure Tween 20 solution at the same concentration. In contrast, if this amount of Tween 20 is injected beneath a previously adsorbed protein layer, the change of σ takes minutes or tens of minutes, depending of the protein concentration.

5. Conclusions

We propose a simple new method for determination of the threshold ("yield") stress of adsorbed protein layers on A/W interface. When this yield stress is overcome, a layer composed of a globular protein (β-lactoglobulin) starts to undergo significant elastic deformation, possibly as a result of breakage of some intermolecular linkages. Our experimental method is based on following the motion of a spherical solid particle which lies on the liquid boundary, when the latter is deformed by raising a barrier attached to it. The method is sensitive to small changes in the layer structure. Increasing protein concentration brings about layer reinforcement and a corresponding increase of the yield stress. Results for the elasticity modulus of adsorbed layers of β-LG are compared with data reported in the literature, and good agreement is found. We believe our method might be a useful tool for studying protein layer rheology.

The presence of low molecular weight nonionic surfactant, Tween 20, leads to a loss of elastic rheological properties of the adsorbed protein layer. Tween 20 either replaces part of the protein or connects to it on the interface, thus breaking the intermolecular bonds responsible for the existence of a gellike network. Complete fluidity (and lack of Hookean elasticity) is observed when Tween 20 and β-lactoglobulin are left to adsorb simultaneously from a mixed solution. When Tween 20 is added to a system with already built interfacial protein layer (of β-LG), the fluidization is gradual and depends on whether the layer is mechanically disturbed or not. These effects are due to the higher surface activity and higher surface pressure of the small surfactant molecules.

Acknowledgment. This work was financially supported by Kraft Foods, Inc. We greatly appreciate the fruitful and stimulating discussions with Prof. Peter Kralchevsky from LCPE.

LA001347I

(24) Kraegel, J.; Wuestneck, R.; Clark, D. C.; Wilde, P.; Miller, R. *Colloids Surf.* **1995,** *98*, 127.
(25) Clark, D. C. In: *Characterization of Food: Emerging Methods;* Gaonkar, A. G., Ed.; Elsevier: Amsterdam, 1995; Chapter 2, pp 23−57.
(26) Dickinson, E.; Euston, S. R. *Prog. Colloid Polym. Sci.* **1990**, *82*, 65.
(27) Courthaudon, J.-L.; Dickinson, E.; Matsumura, Y.; Clark, D. C. *Colloids Surf.* **1991**, *56*, 293.